RESEARCH TRIANGLE INSTITUTE

RTI/3629/90-Quarterly August 1990

SEMICONDUCTOR DIAMOND TECHNOLOGY

Quarterly Report -- First Quarter
1 January 1990 - 31 March 1990

R. J. Markunas
R. A. Rudder
J. B. Posthill
R. E. Thomas

STRATEGIC DEFENSE INITIATIVE ORGANIZATION
Innovative Science and Technology Office

Office of Naval Research
Program No.
N00014-86-C-0460

POST OFFICE BOX 12194 RESEARCH TRIANGLE PARK, NORTH CAROLINA 27709-2194

REPORT DOCUMENTATION PAGE

Form Approved
OMB No 0704-0188

1. AGENCY USE ONLY *(Leave blank)*	2. REPORT DATE	3. REPORT TYPE AND DATES COVERED
	1 November 1990	Quarterly, 1 January 1990 - 31 March 1990

4. TITLE AND SUBTITLE
Semiconductor Diamond Technology

5. FUNDING NUMBERS
N00014-86-C-0460

6. AUTHOR(S)
R.J. Markunas, R. A. Rudder, J. B. Posthill, R. E. Thomas

7. PERFORMING ORGANIZATION NAME(S) AND ADDRESS(ES)
Research Triangle Institute
P.O. Box 12194
Research Triangle Park, NC 27709

8. PERFORMING ORGANIZATION REPORT NUMBER
83U-3629

9. SPONSORING/MONITORING AGENCY NAME(S) AND ADDRESS(ES)
Office of Naval Research
800 N. Quincy Street
Arlington, VA 22217-5000

10. SPONSORING/MONITORING AGENCY REPORT NUMBER

11. SUPPLEMENTARY NOTES

12a. DISTRIBUTION/AVAILABILITY STATEMENT
Approved for public release; unlimited distribution

12b. DISTRIBUTION CODE

13. ABSTRACT *(Maximum 200 words)*

The semiconducting diamond technology development this quarter has concentrated on the continuing advance of a low pressure rf-plasma assisted chemical vapor deposition technique and the advance of the surface chemistry facility. Basic studies of the low pressure rf-plasma assisted CVD system have shown the plasma to be a chemically reactive plasma which converts CH_4 into C_2H_2, produces atomic H, and gasifies graphitic carbon. The power input into the discharge is sufficient to maintain the discharge in the "red" mode where the plasma emission is dominated by atomic hydrogen emission. The atomic hydrogen population is estimated to be at approximately 2500K.

The surface chemistry facility will be an important tool enabling elucidation of CVD processes in diamond growth. Qualifications of the surface chemistry facility has involved significant geometry modifications to reduce hydrogen background in the mass quadrupole and to improve signal collection from the sample surface. These improvements permit the doublet hydrogen desorption spectrum from a Si(100) surface to be delineated.

14. SUBJECT TERMS
Diamond, Semiconductor, Epitaxy, Doping, Chemical Vapor Deposition ~~(CVD)~~

15. NUMBER OF PAGES
22

16. PRICE CODE

17. SECURITY CLASSIFICATION OF REPORT	18. SECURITY CLASSIFICATION OF THIS PAGE	19. SECURITY CLASSIFICATION OF ABSTRACT	20. LIMITATION OF ABSTRACT
UNCLASSIFIED	UNCLASSIFIED	UNCLASSIFIED	

TABLE OF CONTENTS

LIST OF FIGURES

1.0 INTRODUCTION

This is the 1990 First Quarterly Report on the Semiconducting Diamond Program Contract No. N00014-86-C-0460 at Research Triangle Institute.

Previous work had demonstrated both polycrystalline and homoepitaxial growth of diamond at pressures between 0.50 and 10.0 Torr using a low pressure rf-plasma assisted CVD system. Both the polycrystalline and homoepitaxial diamond films exhibited sharp 1332 cm^{-1} Raman signatures with the polycrystalline material also containing varying degrees of non-diamond bonding. Some homoepitaxial films and almost all polycrystalline films exhibited a broad photoluminescence background. The most likely origin of the photoluminescent center is a carbon vacancy defect. Homoeptiaxial films deposited by the low pressure rf-plasma assisted technique at temperatures $\geq$650 °C showed no photoluminescence. These films are indistinguishable from the Raman technique from the substrate itself. Scanning electron microscopy (SEM) of deposited layers show the topography to be extremely planar. Scratch lines remaining from the mechanical polish of the substrate are not apparent on the substrate after film growth. Source gases used in this work were 1% CH_4 in H_2 and 2% CO in H_2. Either source gas is capable of diamond deposition, and mixtures of the two sources were used during some homoepitaxial growths. This quarter, emission and mass spectroscopy have been used to better characterize the growth conditions for diamond deposition in this technique. The plasma is seen to be a chemically reactive plasma creating atomic hydrogen, converting CH_4 into C_2H_2, and gasifying graphite or other solid carbon sources into C_2H_2. The effective electron temperature of the plasma

varies between 3200 and 3420 K depending on the pressure conditions.

Work in the surface chemistry facility has progressed remarkably well. Experiments with atomic H dosing and desorption under the system geometry and configuration last quarter showed the H_2 background in the system to be too high during sample desorptions. As a result the H_2 desorbing from the sample was obscured by the H_2 background. To improve the H_2 desorption signal, two modifications were made to the surface chemistry facility; *first*, to reduce the system background, the sample was directly heated by passing current through the sample which was a heavily doped n-type Si(100) oriented wafer, and *second*, to improve the quadrupole counts from the sample, a quartz shroud with a 4 mm aperture to the sample was placed around the quadrupole to discriminate during the temperature ramp H_2 desorbing from the wafer from H_2 desorbing from the vacuum walls. These changes made dramatic improvements in the mass desorption signal. The system now resolves the β_1 and β_2 desorption peaks from a Si(100):H surface.

2.0 LOW PRESSURE rf-PLASMA ASSISTED CHEMICAL VAPOR DEPOSITION

Diamond chemical vapor deposition using various filament- or plasma-assisted techniques has been clearly demonstrated by numerous workers. Those techniques have typically employed pressures between 20 and 100 Torr with a small percent of hydrocarbon in the gas (0.5 - 2.0%). Recent demonstrations of diamond growth using atmospheric pressure techniques such as the dc plasma jet and the acetylene torch make it evident that diamond growth is not restricted to pressures below 100 Torr. Furthermore, our report of diamond growth at pressures between 1 and 10 Torr using rf excitation and Hiraki's report of diamond growth at 0.100 Torr using electron cyclotron resonance of a microwave discharge show that diamond deposition is not limited to pressures above 20 Torr. While diamond deposition has been demonstrated by a wide variety of processes under extremely different conditions, an understanding of the mechanism of diamond growth, in particular an understanding of diamond nucleation, has not yet been achieved. Even though parametric studies of diamond deposition in the high pressure reactors have been reported, the interdependence of process variables makes interpretation and assignment of causal effects difficult. Studies of diamond deposition at lower pressures should allow a better separation of process parameters and a better understanding of diamond growth.

2.1 Characterization of the Plasma

Two techniques have been used to characterize the plasma discharge, emission spectroscopy and mass spectroscopy.

As discussed in previous quarterly reports, the discharges can be classified in a low power and a high power state. At low rf power levels, the discharge of 1% CH_4 in H_2 is bluish in color and had been designated "blue" mode. In the blue mode, emission from CH swann bands and the antibonding state of molecular H_2 are observed. Transitions from the antibonding state of molecular H_2 to a bonding state occur over a wide frequency range and hence produce a continuum of emission. Statistically, about 5% of antibonding molecular H_2 dissociated into atomic hydrogen. Considering that probably only a small percentage of the neutral H_2 is excited, the "blue" mode is not a very efficient generator of atomic hydrogen.

At higher rf power levels, the impedance of the hydrogen discharge reduces allowing more power coupling to the gas. The discharge becomes instantly red in color. The high power mode of operation has been designated "red" mode in previous quarterly reports. In the red mode, emission from the H_α, H_β, and H_δ, ($n = 3 \rightarrow 2$, $n = 4 \rightarrow 2$, and $n = 5 \rightarrow 2$) states are clearly evident. It is important to note that observed transitions are from atomic hydrogen states and are direct evidence of atomic hydrogen in the plasma.

This quarter, more extensive analysis of the red mode emission has been performed. Figure 2 shows a typical spectrum from a 1% CH_4 in H_2 discharge in the red mode. The H_α, H_β, and H_δ transitions have been noted. One can use the separation of the $n = 2$, 3, and 4 energy states, the statistical weight of each state, the lifetime of each state (τ), and an assumption of a Boltzman distribution for the atomic hydrogen

population to deduce the an effective temperature of the discharge. The basic equations with the statistical weights of each n = 2, 3, and 4 state are shown below:

τ_{3s}	160 ns	τ_{4s}	230 ns
τ_{3p}	5.4 ns	τ_{4p}	12.4 ns
τ_{3d}	15.6 ns	τ_{4d}	36.5 ns
		τ_{4f}	73.0 ns

$$I^{656} = hc\nu_{656}\, N_0/Q\, \{1/\tau_{3s} + 3/\tau_{3p} + 5/\tau_{3d}\}\, \exp(-E_3/kT)$$

$$I^{486} = hc\nu_{486}\, N_0/Q\, \{1/\tau_{4s} + 3/\tau_{4p} + 5/\tau_{4d} + 7/\tau_{4f}\}\, \exp(-E_4/kT)$$

By ratioing the intensities of the 656 nm line to the 486 nm line, one can deduce the effective temperature.

In the growth of diamond by this low pressure technique, the reactor conditions below 10 Torr were selected by maintaining the reactor as a constant chemical reactor. This was attempted by i) reducing the flow rate in proportion with the pressure drop and, hence, keeping a constant residence time in the plasma, ii) adjusting the rf power input so as to be just high enough in power to sustain the red mode. Table I shows that the effective temperature of the discharge remained approximately the same for the pressure series from 1 to 10 Torr. This occurred despite the factor of 6 reduction in rf power input. It is interesting to note that the calculated plasma temperature is close to the filament temperatures used in hot-filament CVD of diamond.

Table I

Pressure	Flow rate (sccm)	Estimated rf power (w)	T_{plasma} (K)
10	12.5	1200	3270
7	8.8	900	3200
5	6.3	500	3200
3	3.8	330	3350
1	1.3	200	3420

Besides emission spectroscopy, mass spectroscopy has been used to establish the effluents of chemical species from the discharge. As can be seen from Figure 1, the mass quadrupole is not located near the discharge but far from the discharge. Hence, the results here do not reflect necessarily the population of the plasma species, but rather the by-products obtained as the hydrogen and methane interact with each other and nearby surfaces as they pass through the discharge. In previous quarterly reports, we had reported the conversion of CH_4 to C_2H_2 as it evolves through the discharge. Figure 2 shows those results. At pressures from 10 to 1 Torr under the same flow rate and power conditions as reported in Table 1, a conversion of CH_4 to C_2H_2 of about 40% is observed with some percentage of the hydrocarbons being depleted from the gas. These experiments were conducted without the graphite stage in the reactor. Figure 3 shows a dramatic difference when the graphite susceptor is inserted near the plasma region. With the graphite stage 3.0 mm below the discharge, C_2H_2 production was observed at levels greater than the original CH_4 counts. Gasification of the graphite stage is a major source of C_2H_2 production in the low pressure regime around 3 Torr. At higher pressures, C_2H_2 production from the graphite is comparable to the

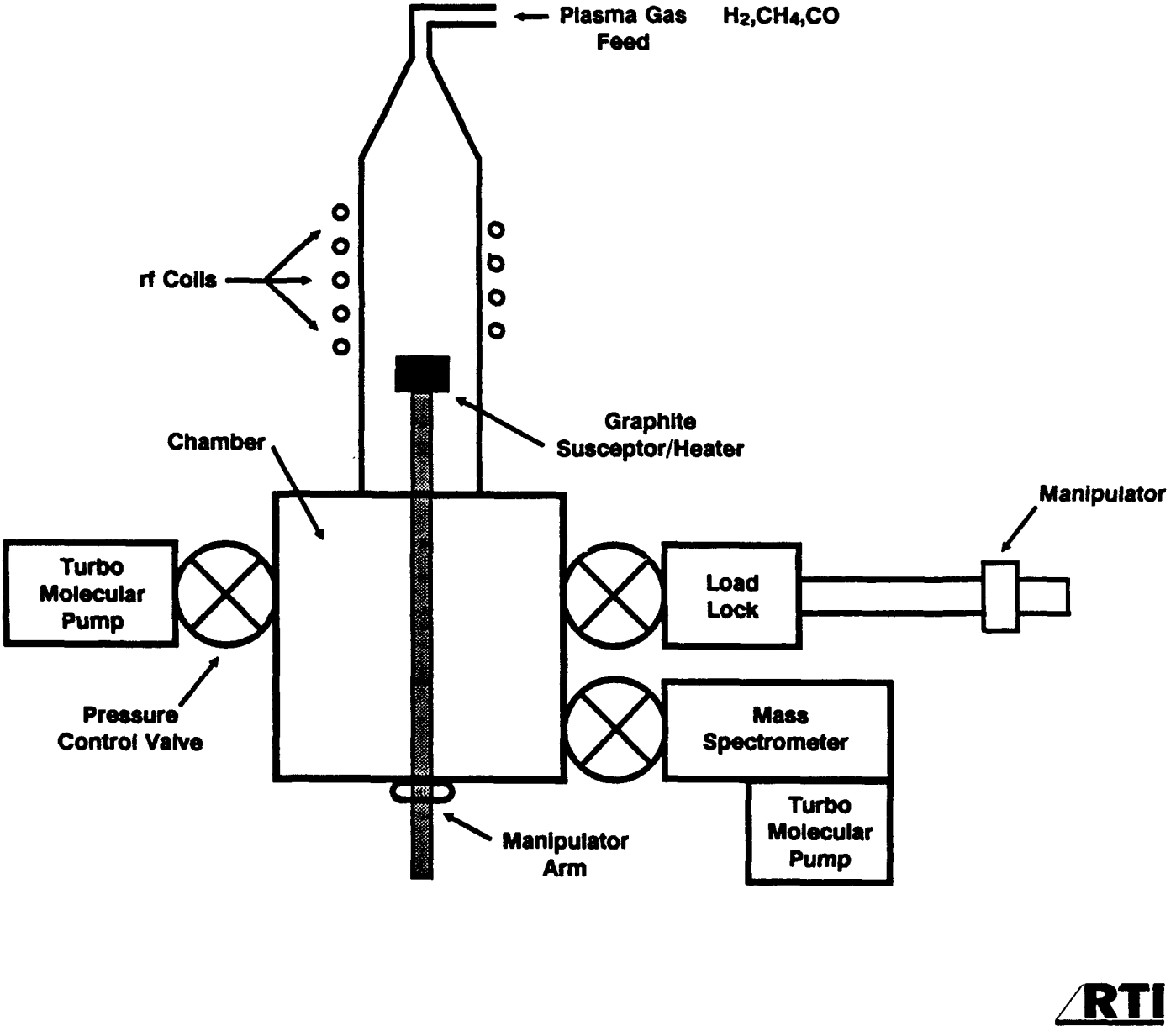

Figure 1. Schematic of low pressure rf-plasma CVD system.

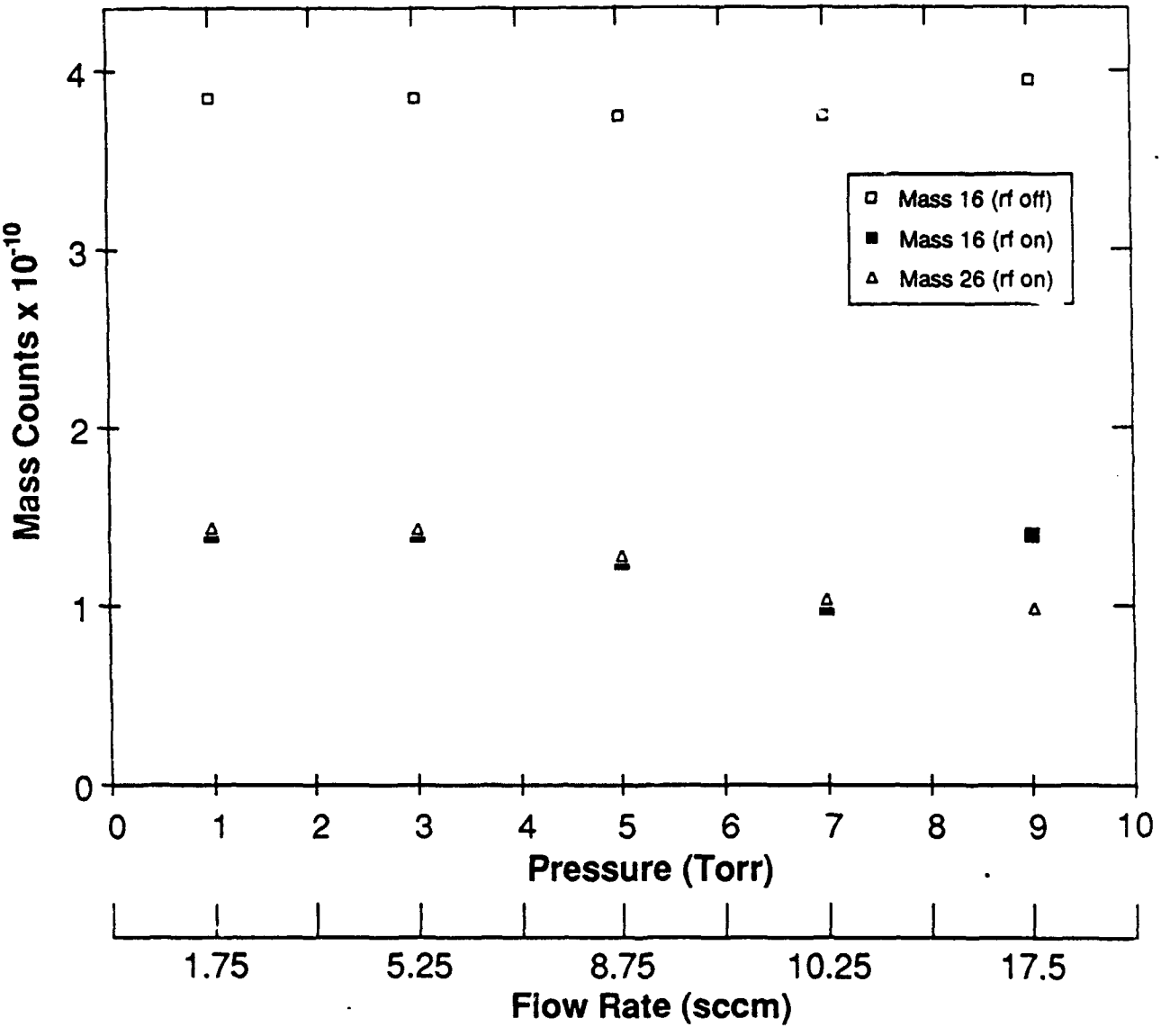

Figure 2. Mass quadrupole sampling of reactive gasses (no graphite susceptor).

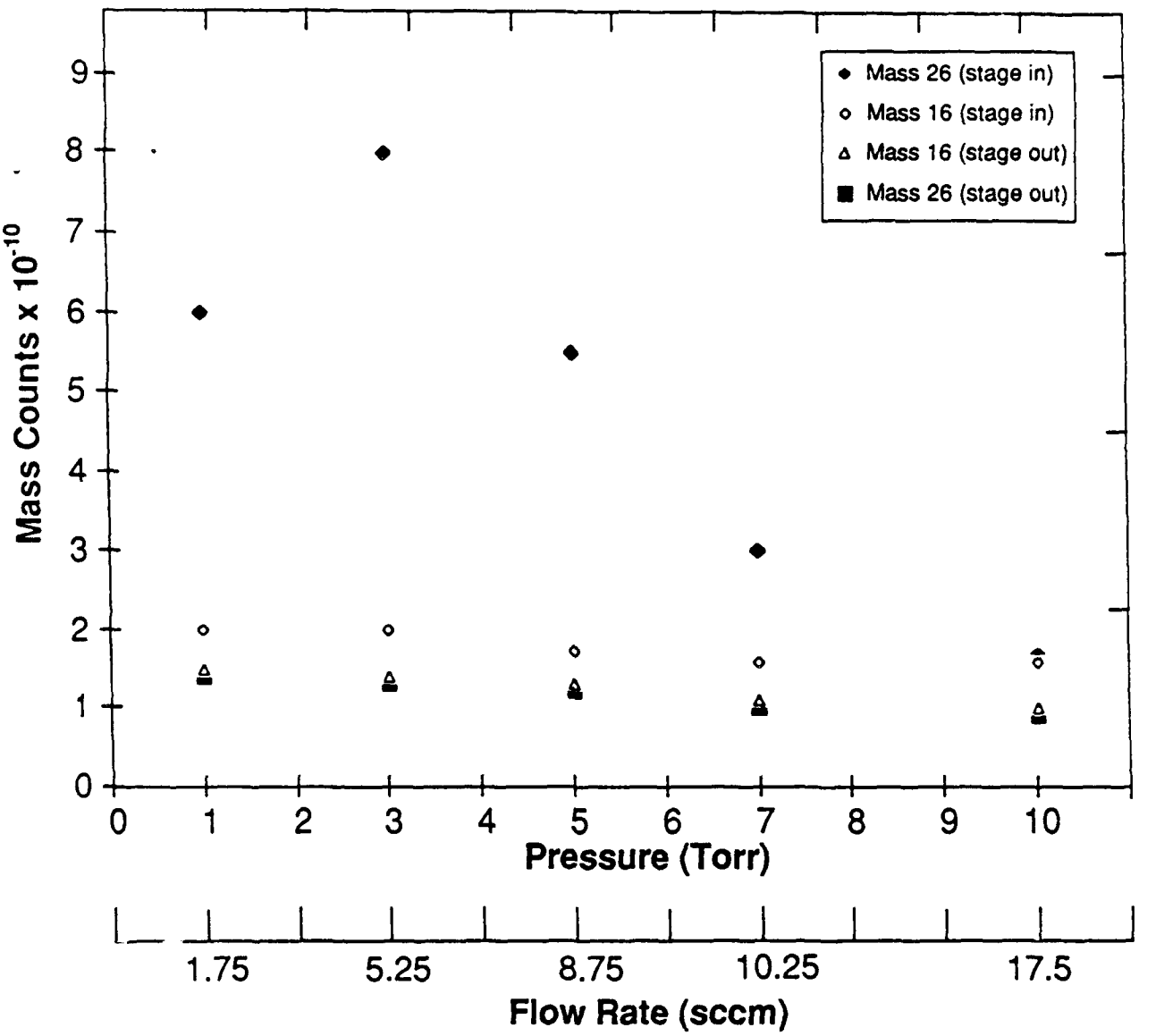

Figure 3. Mass quadrupole sampling of reactive gasses (with graphite susceptor present near plasma).

amount observed from CH_4 conversion to C_2H_2. It is interesting to note that the graphite gasification product is C_2H_2. If the gasification product were CH_4, then one would expect to see the CH_4 as was observed in Figure 3 when CH_4 was introduced into the reactor. The graphite susceptor used in this study is not highly oriented polycrystalline graphite (HOPG) but rather a densified small grain graphite used typically in fabrication of mechanical structures. Work by using filament production of atomic hydrogen has shown that CH_4 is the primary hydrocarbon produced upon gasification of HOPG. Similar results were also reported by Auciello using a discharge source to produce a beam of atomic hydrogen on HOPG. The gasification of a small grain graphite may be more reminiscent of the diamond deposition process where codeposition of graphite is dissolved by the hydrogen. In a codeposition process, it is unlikely that large grain polycrystalline graphite would develop. Rather, small grains of non-diamond material will be dissolved before they could grow larger.

This work has consequences to those workers who are determining gas phase populations of various hydrocarbons under diamond-producing discharges or filaments. Acetylene populations may arise not only from CH_4 conversion but also from gasification of carbon on nearby surfaces. Movement of graphite surfaces towards and away from the discharges or movement of the filament allows determination of whether or not the C_2H_2 is wall produced or gas produced.

2.2 Alternate Cycle Work

Workers at AT&T Bell laboratories reported an interrupted growth cycle whereby the gas mixture was varied from a He - CH_4 to a He - H_2 mixture during each half of the cycle. The He - CH_4 half-cycle deposited material while the He - H_2 mixture was used to etch graphitic sites from the diamond surface, thus, allowing diamond growth to propagate during the subsequent He - CH_4 cycle. This work occurred at 25 Torr, under microwave W excitation. Work at Research Triangle Institute attempted to mimic the diamond growth cycle used by the AT&T group. Furthermore, we hoped to (upon verification of the AT&T process) to grow layers with and without the He - H_2 half-cycle in order to establish the nature of the material prior to and after the He - H_2 half-cycle. Work here was not able to produce high quality diamond films using an alternate cycle process. Figure 4 shows Raman results from a film deposited using a cyclic process. The films displayed no prominent 1332 cm^{-1} line. A feature at 1158 cm^{-1} was observed which is similar to what is observed in other diamond growth facilities as the process parameters are being optimized for diamond production. Electron loss from these films showed no π bonding and did show a 34 eV plasmon loss line characteristic of diamond. No changes in the chemical bonding from Raman analysis or in crystalline regrowth from SEM analysis were observed. Figure 5 shows the SEM appearance of deposited layer which after growing in a He-CH_4 discharge was exposed to a He-H_2 discharge for 30 min. No significant morphological changes were found. The film did etch under the He–H_2 exposure. Films grown with cycles of He–CH_4 and He–H_2 showed similar surface topographies and Raman spectra.

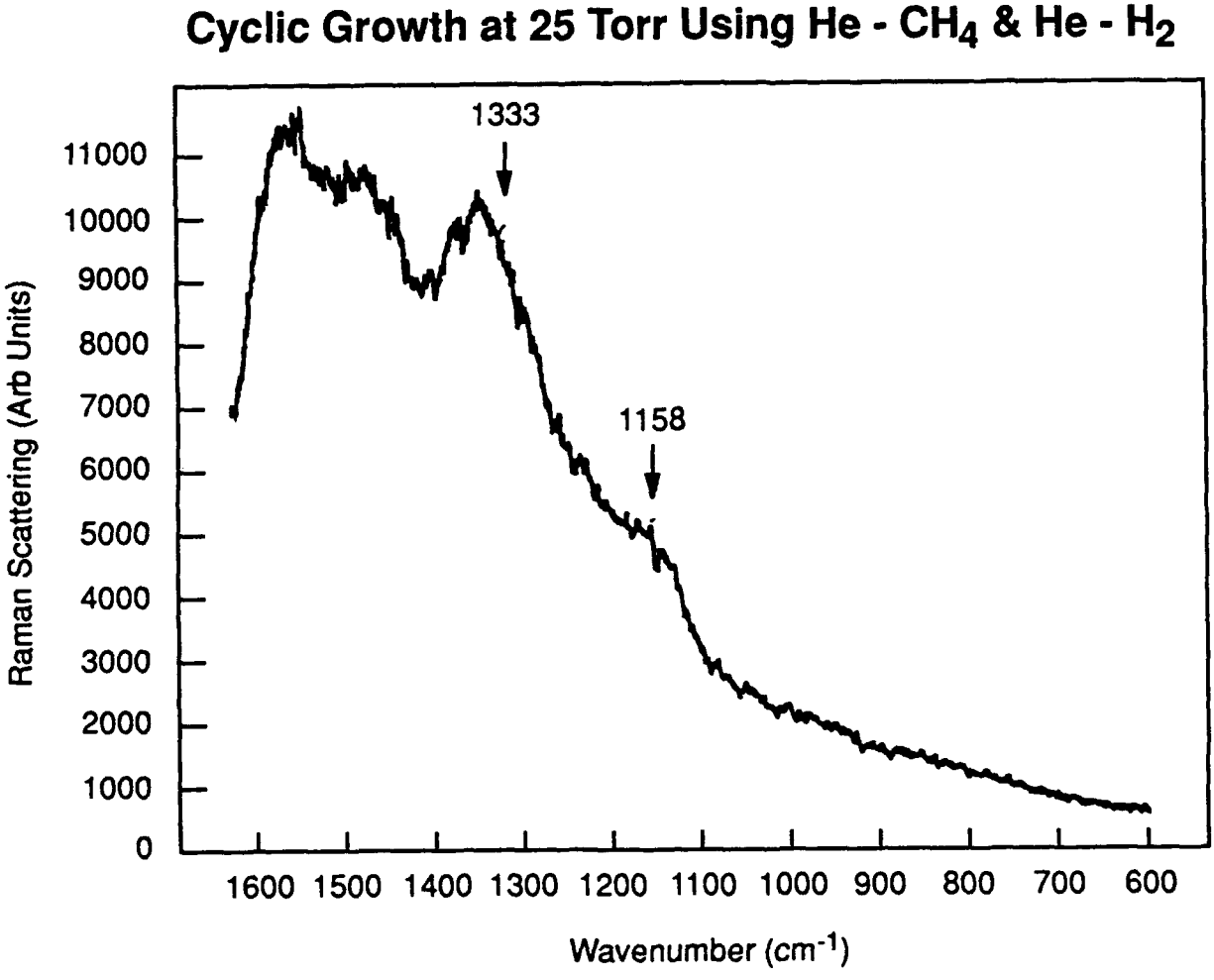

Figure 4. Raman spectrum (taken at NRL, courtesy Jim Butler) of diamond film deposited using cyclic process.

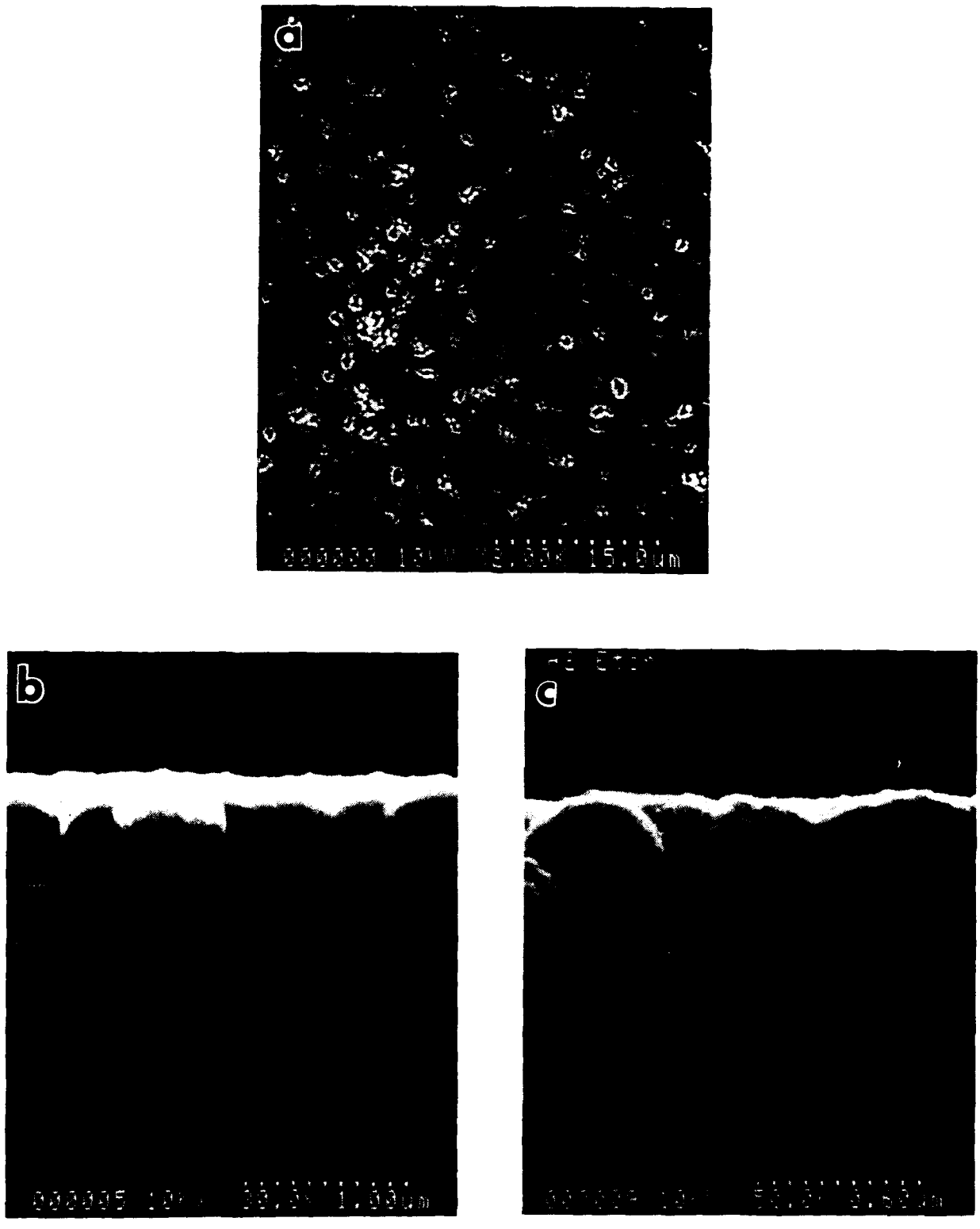

Figure 5. SEM photographs of alternating cycle growth and the result of exposing the sample to a He/H_2 discharge for 30 min.

3.0 PROGRESS IN ALE DEVELOPMENT

A new technique for diamond deposition was derived from work performed at Research Triangle Institute for the purpose of developing a diamond atomic layer epitaxy (ALE) process. While this technique is not an ALE process, it represents an important step away from plasma or filament assisted processes. With this technique, diamond is grown by passing a CF_4, F_2 mixture across a heated substrate (850 °C). The F_2 is decomposed at this temperature and can readily dissolve graphite from the growth surface allowing diamond sites to dominate the surface. CF_4 was added as the source gas for diamond deposition. The homoepitaxial layer showed excellent surface topography and sharp 1332 cm^{-1} Raman line. Experiments with the CF_4/F_2 process have been limited by the need to pre-deposit carbon on the reactor walls for substantial amounts of time to avoid metal incorporation in the films. The metal contamination derives from fluorine-etch and vapor transport from the walls to the depositing film. The CF_4/F_2 process may indeed be convoluted by fluorine reactions with the hydrogenated carbon deposits on the walls of the reactor. Hydrogen transported from the hydrogenated wall deposits may be playing a critical role in the process. Experiments with mixed fluorocarbons-hydrocarbons should yield insight into that process.

Understanding of the CF_4/F_2 processes, the nucleation and growth phenomena, and development of diamond ALE scenario will be assisted by the recent upgrade to the surface-chemistry facility. The surface chemistry facility has a mass quadrupole, a gas doser, and a ramped temperature stage for performing thermal mass desorption experiments. Preliminary experiments in H_2 desorption revealed that the H_2

background in the chamber was too high to allow detection of H_2 that was desorbing from the sample during temperature ramp. To improve the H_2 desorption signal from the Si, two modifications were made to the surface chemistry facility. *First*, to reduce the system background, the sample was directly heated by passing current through the sample which was a heavily doped n-type Si(100) oriented wafer. Previously, the sample was heated radiatively by a tantalum element. Heating of the sample resulted in outgassing of the heater stage and other fixtures receiving radiative flux. *Second*, to better discriminate flux desorbing on the sample surface from flux desorbing on chamber fixtures, a quartz shroud with a 4 mm aperture to the sample was placed around the quadrupole assembly. These changes made dramatic improvements in the mass desorption signal.

Analytical facilities on the surface chemistry chamber included an Extrel C-50 quadrupole mass spectrometer, Princeton Research Incorporated LEED/Auger apparatus, and an Ircon 15C10 infrared pyrometer with a temperature range of 200 - 800 °C. Silicon samples used in this work were cleaved from 3" (100), heavily doped n-type, .005 ohm-cm, wafers. The wafers had been factory polished on both sides. Polishing on the backside gave more reproducible results for the pyrometric temperature measurements. Samples were cleaved to 1 cm $\times$ 3 cm, dipped in HF for 2 minutes, rinsed in DI water for 5 minutes, and then clamped into the heating fixture. The chamber was then evacuated and baked for 2-3 days. Further cleaning of the sample was accomplished in-situ by thermal annealing. The sample was flashed at successively higher temperatures, taking care to keep the pressure as low as possible--

typically $< 2 \times 10^{-8}$ Torr. Good 1×2:2×1 LEED patterns were obtained using this procedure. A W filament at approximately 2000 °C was used for the production of atomic hydrogen. The filament was located 2-3 cm from the silicon surface. Gas flow was controlled with a leak valve and gas was introduced into the chamber through a 6 mm S.S. tube located 3 cm behind the W filament. Dose rate was set by measuring the chamber pressure, noting the leak valve setting, and dosing for a predetermined time.

After dosing the sample was moved in front of the quadrupole for thermal desorption. The sample temperature was measured with an Ircon IR pyrometer which had been calibrated with a thermocouple attached to a silicon wafer.

Figure 6 shows a typical thermal desorption spectrum after dosing with atomic hydrogen. The desorption peaks are still seen on top of a substantial hydrogen background but the β_1 and β_2 peaks are clearly resolved. The predominant desorption product we see after dosing silicon with atomic hydrogen is molecular hydrogen. We have also monitored masses 29, 30, 31 (SiH, SiH_2, SiH_3), but have not detected desorption products for these species. Gates et. al. finds that approximately 4% of surface hydrogen desorbs as $SiHi_4$ resulting in removal of about 1% of a monolayer of Si atoms. Higher order silanes are also found but at a much smaller concentration; accounting for about 0.001 of a monolayer of Si. Production of silanes decreases with increasing adsorption temperature.

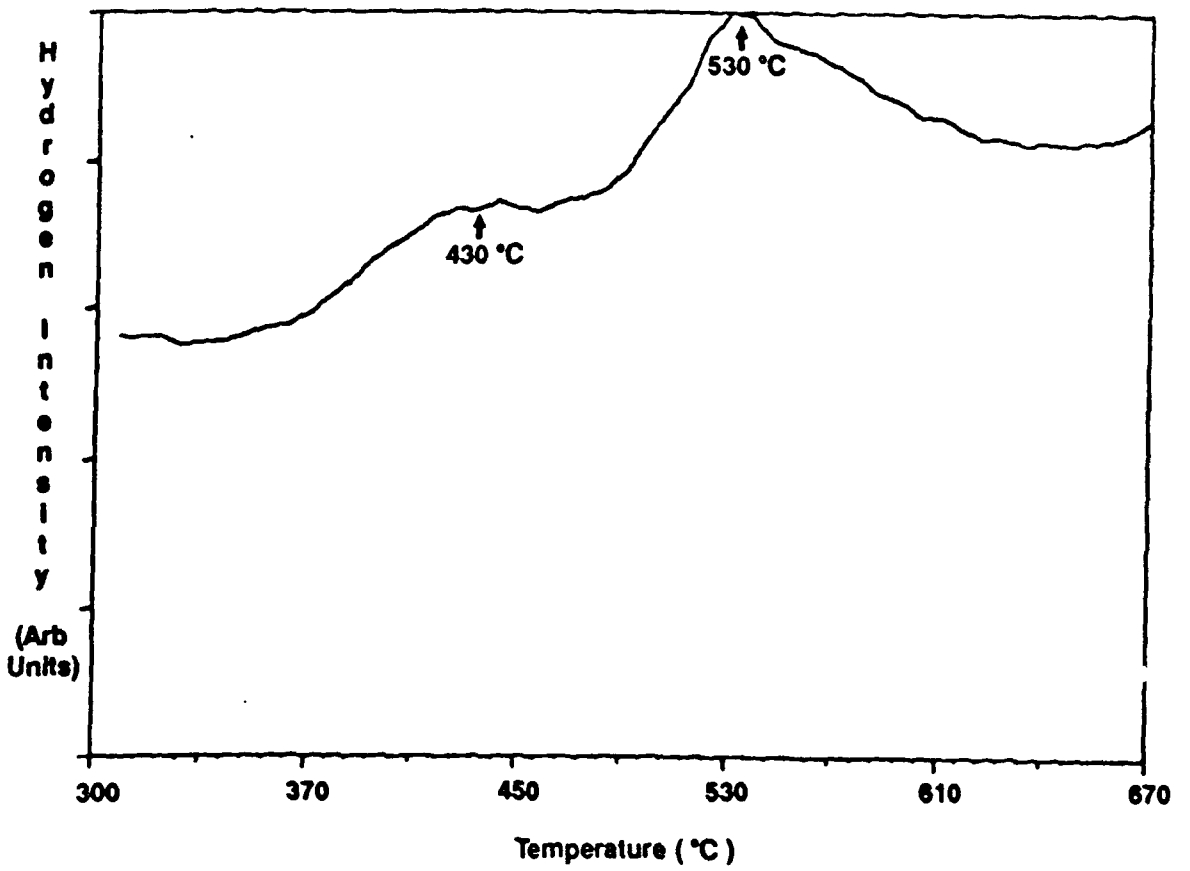

Figure 6. H_2 desorption from a Si(100) 1×1:H surface.

Hydrogen desorption temperatures we have seen are 410-440 °C for the β_2 peak and 535 - 580 °C for the β_1 peak. The literature values are 425 and 540 °C respectively. As hydrogen is added to the Si 2×1 surface, the dimer sites fill up. Eventually, the hydrogen causes the dimer bonds to break and bond to the hydrogen. The β_2 peak, at a lower temperature than the $\beta 1$, is the first hydrogen to desorb from the silicon atom. The surface then reconstructs and the second hydrogen atom desorbs. We see the surface reconstruction change from 2×1 to 1×1 with the addition of atomic hydrogen.

A second series of experiments was performed using molecular hydrogen as the dosing gas instead of atomic hydrogen. Molecular hydrogen does not appear to adsorb on the surface as we see no evidence of changes in the 2×1 LEED pattern. In addition the thermal desorption shows no indication of the β_1 and β_2 peaks.

4.0 CURRENT DIRECTION OF RESEARCH

Current research is examining the area of nucleation with new research tools such as the surface chemistry facility and new strategies. Epitaxial overgrowth of diamond on Ni is soon to be evaluated. Thin epitaxial Ni layers (150-500 Å) have been deposited on diamond substrates, and holes have been etched in the Ni to provide seeds upon which diamond can nucleate and overgrow. Preferential growth directions will be determined by observing the diamond growth fronts propagating across the Ni layer. Extension of the CF_4/F_2 process to explore other source gases such as $C_2Cl_2F_2$ and $C_2H_2F_2$ in conjunction with the F_2 will be undertaken. Doping studies will concentrate on controllable p-type doping for eventual fabrication of some simple FET test transistors. Solid phase regrowths are being conducted jointly with Max Swanson and Nalin Parikh at UNC/CH. Experiments have been designed to determine the temperature threshold for overgrowth and the maximum damage the crystal can withstand before regrowth is inhibited. Effects of F on the regrowth is to be evaluated by ion implanting F^+ ions prior to regrowth. The doses can be adjusted to yield comparable damage.